Knockdown of BMI1 is sensitive to Paclitaxel in cervical and endometrial cancer

Yiting Zhao (958712057@qq.com)
The Affiliated People's Hospital of Ningbo University https://orcid.org/0000-0002-3526-2321
Yan Lin
The Affiliated People's Hospital of Ningbo University
Weili Yang
The Affiliated People's Hospital of Ningbo University
Jun Chen
The Affiliated People's Hospital of Ningbo University
Xiaofeng Jin
Ningbo University Medical School https://orcid.org/0000-0003-0801-8638

Research Article

Keywords: cervical cancer (CC), endometrial cancer (EC), BMI1, Overexpression, Paclitaxel (PTX)

Posted Date: February 27th, 2023

DOI: https://doi.org/10.21203/rs.3.rs-2599518/v1

Abstract

Background

BMI1, a critical member of the Polycomb Repressor Complex 1, plays a key role in regulating cell proliferation, differentiation, and senescence; however, abnormal expression of BMI1 is associated with the occurrence and progression of tumors, chemotherapeutic resistance, and poor prognosis.

Methods

In this study, we used the TCGA and CPTAC database to analyze the mRNA and protein expression of BMI1 in cervical and endometrial cancer. Next, we analyzed the protein expression level of BMI1 in 40 pairs of human cervical cancer (CC) tissue samples and 12 pairs of endometrial cancer (EC) tissue samples by IHC Analysis. Western blotting and RT-qPCR were used to detect the changes of mRNA and protein levels in CC and EC cells after BMI1 knockdown. Additionally, the function of BMI1 in CC and EC cancer cells were studied through cell functional experiments. Finally, we assessed the synergic anti-growth effect of shBMI1 combine with paclitaxel (PTX) treatment by assay.

Results

Mining the data from TCGA database, the mRNA level of BMI1 was significantly high in several malignant tumors, but not in CC and EC. However, through the TCGA database, high mRNA levels of BMI1 were associated with the pathological type of CC, and high protein levels of BMI1 were related to the pathological type and tumor grade of EC via the CPTAC database. Furthermore, the BMI1 protein level is overexpressed in cancer tissues of CC and EC compared with normal tissues, as detected by IHC analysis, and the clinical data indicate that the expression of BMI1correlates with the pathological differentiation of the two cancers. Additionally, we showed that high expression of BMI1 in vitro promoted the proliferation and migration of CC and EC cells. Moreover, CC and EC cells with low BMI1 expression were more sensitive to the paclitaxel (PTX).

Conclusions

Our results show that BMI1 is overexpressed in the tumor tissues of CC and EC patients and provides potential information for the treatment of PTX by targeting the oncogenic protein BMI1 in patients with high BMI1 expression.

Introduction

Cervical cancer (CC) and endometrial cancer (EC) are two of the most common gynecologic malignant tumors in China and worldwide. CC in China accounts for 12% of the worldwide incidence of cervical

cancer and 11% of cervical cancer-related deaths[1]. Globally, there were 382,000 new EC cases and 90,000 deaths in 2018, with an increasing incidence and decreasing age of onset[2; 3]. Although the strategies for the treatment of CC and EC are both based on clinical evaluation and stage, the primary treatment is surgery or chemoradiotherapy for early or locally advanced stages2,3[4; 5]. Paclitaxel (PTX)-based drugs are the main chemotherapy regimen for advanced stages of CC and EC patients; however, this treatment strategy is effective in the beginning, but with drug resistance and adverse reactions observed[6].

BMI1, an important member of the Polycomb Repressor Complex 1 (PRC1), regulates gene silencing by restructuring chromatin conformation and is abnormally expressed in different types of cancer. Its expression is associated with occurrence, progression, and poor prognosis[7–12]. Although several studies have indicated that inhibition of BMI1 may be a therapeutic approach in both CC and EC[12–16], there is still lack the evidence from clinic data of CC and EC patients and the relationship between BMI1 and PTX-associated drug resistance.

Here, we demonstrated that BMI1 protein levels are significantly elevated in CC and EC patient tumors. In a cell model of CC and EC, high BMI1 expression triggered the proliferation and migration of CC and EC cells, while low BMI1 expression inhibited these phenomena. In addition, PTX and BMI1 knockdown significantly suppressed cell proliferation. Therefore, using PTX-based drugs combined with targeting BMI1 may serve as a promising approach for CC and EC patients with high BMI1 levels.

Materials And Methods

Patients and clinicopathological data

A uniformly standardized pan-cancer dataset from The Cancer Genome Atlas database (TCGA) database (PANCAN, N = 10535, G = 60499) was downloaded from the UCSC platform (https://xenabrowser.net/), and the expression data of ENSG00000168283 (*BMI1*) gene in 26 cancer species (GBM, GBMLGG, LGG, CC, LUAD, COAD, COADREAD, BRCA, ESCA, STES, KIRP, KIPAN, STAD, PRAD, EC, HNSC, KIRC, LUSC, LIHC, THCA, READ, PAAD, PCPG, BLCA, KICH, and CHOL) were extracted and analyzed. The sample selection criteria were as follows: Normal Solid Tissue, Primary Blood Derived Cancer-Peripheral Blood, Primary Tumor. Log2 (x + 1) conversion for each expression Tumor species with fewer than three samples in a single tumor species were eliminated, and the expression data of 26 tumor species were obtained. R software (Version 3.6.4) was used to calculate the difference in expression between normal and tumor samples in these 26 tumors, and unpaired Student's t-test was used for difference significance analysis.

The mRNA expression of BMI1 in 304 CC and 546 EC cases was downloaded from the UCSC platform(https://xenabrowser.net/)(project:TCGA-CESC/TCGA-UCEC,datatype:RNA-COUNTS). R software (version 3.6.4) was used to calculate the mRNA level differences in *BMI1* between normal and tumor samples in CC and EC (R program: limma; ggplot2; ggpubr). R software (version 3.6.4) was used to calculate pairwise expression differences between paired normal and tumor samples in CC and EC

tumors (R limma; ggpubr). Unpaired Wilcoxon Rank Sum and Signed Rank Tests were used to analyze the significance of differences.

Correlation analysis between *BMI1* mRNA levels and clinical features of CC and CE was performed using the UALCAN platform (http://ualcan.path.uab.edu/index.html) (data type: TCGA database-UCEC/TCGA database-CESC, project: RNA-COUNTS).; Correlation analysis between BMI1 protein expression and clinical features of CC and CE was performed using the UALCAN platform (http://ualcan.path.uab.edu/analysis-prot.html) (data type: CPTAC-UCEC project: BMI1 (NP_005171.4:S251)).

IHC analysis

Forty pairs of human CC tissue specimens and twelve pairs of EC tissue specimens were collected from The Affiliated People's Hospital of Ningbo University. The samples were obtained via surgical excision or biopsy. The selection criteria were as follows: i) the samples were confirmed to be primary CC and EC by pathological diagnosis and ii) the patient had no history of other systemic malignancies. All patients provided signed informed consent, and the study was approved by the Ethics Committee of the Ningbo University School of Medicine.

Formalin-fixed tissue samples from the patients were cut into tissue blocks at room temperature. The tissue blocks were fixed with 4% paraformaldehyde for more than 24 hours, and then dehydrated in ethanol of different concentrations, embedded in paraffin, and sectioned into 4μm slices. Sections were dewaxed and hydrated in xylene and ethanol at different concentrations. Heat-mediated antigen recovery was performed on the sections using Tris-EDTA antigen retrieval solution (Biosharp, BL617A). An ultrasensitive S-P (Rabbit/Mouse) IHC Kit (Kit-9710, Fuzhou Mai Xin Biotechnology) was used for the next steps. Endogenous peroxidase activity was blocked with 3% H_2O_2 at room temperature. Next, the sections were sealed with 10% donkey serum for 15 minutes, mixed with BMI1 antibody (dilution 1:50; Abcam, AB32160), and incubated overnight.

The sections were then treated with biotinylated goat-anti–rabbit/mouse IgG secondary antibodies (Fuzhou Maixin Biotech) for 30 minutes. The sections were then incubated with streptavidin and horseradish peroxidase (Fuzhou Maixin Biotechnology) for 1 hours. Finally, 3,3 '-diaminobenzidine (DAB-0031, Fuzhou Mailxin Biotechnology Co., Ltd.) was used for 1 minutes of staining. Each step was washed three times with 1×PBS for three times, 5 minutes each time. 1xPBS instead of the BMI1 antibody was used as a negative control. Two independent pathologists scored the sections by IHC staining. A semi-quantitative method was used to calculate the percentage of positive cells: ≤10%, 0 points; 11%-25%, 1 point; 26%-50%, 2 points; 51%-75%, 3 points; and > 75%, 4 points. Dyeing degree score: colorless, 0 points; light yellow, 1 point; brown-yellow, 2 points; brown, 3 points; according to the sum of the two, 0 is divided into (-); 1–2 are divided into (+); 3–4 are divided into (+ +); 5–6 are divided into (+ + +); and 7 points (+ + + +). Statistical analysis (-) was negative, (+) and (+ +) combined for weakly positive, and (+ + +) and (+ + + +) combined with strong positive expression. Images were captured using an Olympus IX73 inverted fluorescence microscope and the accompanying software.

Cell lines and cell culture

The human embryonic kidney cell line (HEK-293T) and cervical CC line (HeLa) were obtained from American Type Culture Collection (ATCC). The human EC cell line (HEC-1-A and SPEC-2) is a gift from Professor Kun Gao of Tongji University (Wen et al., 2020). HEK-293T and HeLa were cultured in Dulbecco's Modified Eagle Medium (DMEM, Meilunbio) with 10% Fetal Bovine Serum (FBS Premium, PAN-Seratech). HEC-1-A and SPEC-2 were cultured in Dulbecco's Modified Eagle Medium: Nutrient Mixture F-12 (DMEM/F-12(1:1), Meilunbio) with 10% Fetal Bovine Serum (FBS Premium, PAN-Seratech). All cells were grown at 37°C with 5% CO2.

Similar to our previous study[17], the BMI1 gene fragment was obtained from the cDNA sequence of HeLa cells using specific primers, and the BMI1 fragment and mammalian expression vector pCMV-Myc vector were excised using restriction endonucleases to obtain Kpn1/Not1 sticky ends. This fragment was ligated into the vector to construct the pCMV-Myc-BMI1 plasmid. To achieve knockdown of the target gene, the shRNA sequence targeting BMI1 was sub-cloned intro pLKO.1-GFP-shRNA vectors. Primers and shRNA sequences are listed in **Table S1**. All constructs were verified by DNA sequencing.

All transfection experiments were performed using Lipo6000™ transfection reagent (cat#C0526; Beyotime, China), according to the manufacturer's instructions. Briefly, 10^5 cells were seeded in 6-well plates and transiently transfected with 3 μg of pCMV-Myc-BMI1, shBMI1, or empty vector.

Western blotting

Protein samples from each lysate of fresh cells treated with RIPA buffer (cat#R0010; Solarbio, China) were loaded and separated by 10% SDS-PAGE, and then transferred to Amersham Protran 0.2μm nitrocellulose membranes. NC membranes were blocked with 5% fat-free milk for 1 h at room temperature. The membranes were probed with anti-BMI1 (ab269678; Abcam, England) and anti-GAPDH (cat#A19056, Abclonal, China) at 4°C overnight. The membranes were then incubated with HRP-conjugated anti-mouse or anti-rabbit immunoglobulin (cat#SA00001-1 and cat#SA00001-2; proteintech, America) for 1 hour at room temperature. Proteins of interest were visualized using an enhanced chemiluminescence (ECL) system (cat#412; Vazyme, China). WB was performed 2–3 times in at least two independent experiments, and representative pictures are shown.

Reverse transcription-quantitative PCR (RT-qPCR)

Total RNA was isolated from HeLa, HEC-1-A, and SPEC-2 cells using TRIzol Reagent (cat#15596018; Thermo Fisher, USA), and cDNA was reverse-transcribed using HiScript III All-in-one RT SuperMix Perfect for qPCR (cat#R333; Vazyme, China) following the manufacturer's instructions. PCR amplification was performed using the Taq Pro Universal SYBR qPCR Master Mix (cat#Q712; Vazyme, China). All quantifications were normalized to the level of the endogenous control GAPDH. The primer sequences used for RT-qPCR are listed in **TableS1**. RT-qPCR was performed 2–3 times in at least two independent experiments, and representative pictures are shown.

Wound-healing closure assay

Cells were cultured in 6-well plate, and when the cells grew until they spread over the small wells, the linear wound was scratched with the tip of a 10 μL pipette. The medium was replaced with 2% FBS serum, a proliferation inhibitor (mitomycin C, GlpBio, USA) was added, and wound healing was observed under a microscope and photographed. After 24 and 48 hours, wound healing was again observed under a microscope and photographed, and the degree of wound healing was statistically analyzed. Each analysis was performed in 3 replicates.

Transwell migration assay

Cells transfected with pCMV-Myc-BMI1, shBMI1, or the empty vector were cultured for 24 hours. The cells were digested into a uniform single-cell suspension and centrifuged at 1000rpm for 4 mintues. The cell suspension was centrifuged at 1000 rpm for 4 mintues. The supernatant was discarded and the cells were resuspended in 1 ml of DMEM, counted on a cell counting plate, and diluted with DMEM as needed. Then, three transwell chambers were placed into a 24-well cell plate, and 200 μL of the above single-cell suspension was added to the upper chamber to quantify 1×10^4 cells. Complete medium (500 μL) was added to the lower chamber and the plate was placed in a constant-temperature incubator after standing for 30 mintuesn. After 48 hours, the medium was discarded and the cells were washed twice with PBS. Next, 500 μL of 4% paraformaldehyde fixing solution was added to the chamber and allowed to stand for 30 min. The fixing solution was discarded, the cells were washed twice with PBS, 500 μL of 0.1% crystal violet dye was added, and the plate was stained on a shaker for 20 mintues. After rinsing with PBS three times, the chamber was dried naturally, photos were taken, and statistics were obtained. Statistical analysis were performed using one-way ANOVA). *$P < 0.05$

Cell proliferation assay

The Cell growth curves were determined using the CCK-8 assay. Cell proliferation rates were determined using a Cell Counting Kit-8 (CCK-8) (cat#K1018; APExBIO, America) according to the manufacturer's protocol. Cells were seeded in 96-well plates at a density of 2000 cells per well. On each of the seven consecutive days of seeding, 10 μL of CCK-8 solution was added to each cell culture and incubated for 2 hours. The resulting color was measured at 450 nm wavelength using a microplate absorbance reader (Bio-Rad, Hercules, CA, USA). Each measurement was performed in triplicates.

Colony formation assay

A total of 1500 cells in 2 mL of growth medium were plated in quadruplicate in a 6-well plate, and the growth medium was changed every 3–4 days. After 14 days, the cells were rinsed twice with PBS, fixed with 10% formaldehyde, and stained with crystal violet (cat# G1063; Solarbio, China). The number of colonies was counted. Each count was performed in triplicates.

Statistical analysis

Statistical calculations were performed using GraphPad Prism software. Data are presented as mean ± SD for experiments performed with at least three replicates. The differences between two groups were analyzed using Student's t-test, and multiple comparisons were performed using two-way analysis of variance (ANOVA). Statistical calculations of the transwell assay were performed using one-way ANOVA. Statistical calculations of IHC were performed using SPSS software. The Chi-squared test was used to analyze the differences between the two groups. * represents $P < 0.05$; ** represents $P < 0.01$; *** represents $P < 0.001$.; **** represents $P < 0.0001$.

Ethical statement

All patients participating in the experiment provided signed informed consent, and the study was approved by the Ethics Committee of the Ningbo University School of Medicine.

This article does not contain any studies with animals performed by any of the authors.

Results

1.1 The mRNA level of BMI1 in human cancers from TCGA database

Through TCGA database data analysis, we identified BMI1 as an oncogene in several human cancers, including COAD, COADREAD, BRCA, ESCA, STES, STAD, HNSC, LIHC, and CHOL **(Figure. S1, Table S2)**. We further analyzed the mRNA levels of BMI1 in CC and EC tissues. We compared BMI1 mRNA levels in 304 CC tumor specimens, 3 healthy cervical tissue specimens, 546 EC tumor specimens, and 35 healthy endometrial tissue specimens from TCGA database. The former showed no statistical difference owing to the small number of healthy cervical tissue specimens **(Figure. S2A)**, whereas the mRNA level of BMI1 was significantly higher in normal endometrial tissues than in EC tissues **(Figure. S2B)**. Furthermore, the mRNA level of BMI1 in paired CC and EC samples from TCGA database was also analyzed, with no significant difference in the transcriptional level between normal and tumor tissues **(Figure. S2 C, D)**.

1.2 The correlation between BMI1 and clinical features in CC and EC from TCGA database

The UALCAN platform (http://ualcan.path.uab.edu/index.html) was used to analyze the correlation between BMI1 mRNA level and tumor stage and pathological type in CC and EC patients from the TCGA database (data type: TCGA-UCEC/TCGA-CESC, project: RNA-COUNTS). The transcription level of BMI1 was not significantly correlated with the tumor stage of CC but was related to the pathological type of CC. BMI1 mRNA levels were significantly increased in the endometrioid adenocarcinoma subtypes **(Figure. 1A, B)**. However, in EC, the transcription level of BMI1 was not significantly correlated with tumor stage or the pathological type of EC **(Figure. 1C, D)**.

The UALCAN platform (http://ualcan.path.uab.edu/analysis-prot.html) was used to analyze the correlation between BMI1 protein expression and EC clinical features from the CPTAC database (data

type: CPTAC-UCEC, project: BMI1 (NP_005171.4:S251)), and the results showed that BMI1 protein is highly expressed in endometrioid carcinoma and serous carcinoma subtypes compared with normal tissues **(Figure. 1E)**. In addition, higher BMI1 expression was associated with a high tumor grade in patients**with EC (Figure. 1F)**. However, data on the expression of the BMI1 protein in CC were not found in the CPTAC database.

2.1 Protein level of BMI1 in CC and EC tissues

Since the mRNA level of BMI1 in CC and EC samples from TCGA database exhibits no significant difference, the protein level of BMI1 indicates potential clinical value. We next attempted to detect the expression level of BMI1 protein in CC and normal tissues using IHC analysis. BMI1 protein expression levels were significantly higher in CC tissues than in normal tissues ($\chi2=25.1$, $P<0.001$) **(Figure. 2A, B)**. A total of 52.5% (21/40) of CC tissues exhibited high expression of BMI1, whereas the other CC tissues (47.5%, 19/40) had negative or low expression levels of BMI1. In contrast, 2.5% (1/40) of normal CC tissues exhibited strong staining for BMI1 and 97.5% (39/40) exhibited negative and low staining.

Similarly, BMI1 protein expression levels were significantly higher in EC tissues than in normal tissues ($\chi2=11.06$, $P<0.01$) **(Figure. 2C, D)**. A total of 75% (9/12) of EC tissues exhibited high BMI1 expression, whereas the other EC tissues (25%, 3/12) had negative or low expression levels of BMI1. In contrast, 2.5% (1/12) of normal EC tissues exhibited strong staining for BMI1 and 97.5% (11/40) exhibited negative and low staining. These findings indicated that BMI1 protein expression in CC and EC tissues was higher than that in normal CC and EC tissues.

2.2 Clinical value of BMI1 in CC and EC

The possible correlations between BMI1 protein expression and clinicopathological features in CC and EC tissues were evaluated. The protein level of BMI1 in CC tissues was closely related to the degree of pathological tumor differentiation ($\chi2=10.455$, $P<0.05$). There was no significant correlation with clinicopathological characteristics (age, height, weight, BMI, tumor size, tumor invasion depth, pathological type, TNM stage, FIGO stage, ER expression, and PR expression) (**Table 1**). In EC tissues, the expression level of BMI1 was not significantly correlated with clinicopathological characteristics (tumor pathological differentiation degree, age, height, weight, BMI, tumor size, tumor invasion depth, pathological type, TNM stage, FIGO stage, ER expression, and PR expression) (**Table 2**).

3.1 High expression of BMI1 promotes migration of CC and EC cells

To determine the potential functional role of BMI1 in CC and EC cell lines, we utilized the HeLa, HEC-1-A and SPEC-2 cell lines, and transfected myc-BMI1 and shBMI1 into these cells to increase the expression level of BMI1 or decrease the expression level of BMI1, respectively. The efficiency of shBMI1 was first detected in HEK293T cell, and shBMI1#2 (referred to as shBMI1 in the following text) was chosen for the subsequent BMI1 knockdown experiments because of the best knockdown outcome (**Figure.S3)**. The further BMI1 expression was assessed using RT-PCR and WB, and the results showed that BMI1 mRNA

was significantly increased in HeLa, HEC-1-A and SPEC-2cells after transfection with myc-BMI1, and decreased after transfection with shBMI1 **(Figure. 3A, Figure. 4A, Figure.S4A);** accordingly, the BMI1 protein was consistent with BMI1 mRNA **(Figure. 3B, Figure. 4B, Figure.S4B)**. After the transfection of cells with myc-BMI1 and shBMI1, the effect of BMI1 on cell migration was assessed using a wound-healing closure assay. The results showed that after 24 hours of culture, high expression of BMI1 promoted the migration of HeLa cells, whereas downregulation of BMI1 significantly reduced the migration of HeLa cells **(Figure. 3C)**. However, wound healing assays were not performed in HEC-1-A and SPEC-2 cells because they could not be fully fused in 6-well plate. In addition, the same results were obtained from the transwell migration assay **(Figure. 3D)**. Similar results of the transwell migration of HEC-1-A cells were found, further proving the role of BMI1 in the migration of CC and EC cells **(Figure. 4C)**.

3.2 High expression of BMI1 in vitro promotes the growth and proliferation of CC and EC cells

The results of the CCK-8 assay showed that cell growth and proliferation were increased in myc-BMI1-transfected cells but decreased in shBMI1#2-transfected HeLa, HEC-1-A, and SPEC-2 cells compared with the respective controls **(Figure. 3E, Figure. 4D, Figure.S4C)**. In addition, the results of the HeLa, HEC-1-A, and SPEC-2 cell colony formation assays showed that high expression of BMI1 promoted cell growth and proliferation, and low expression of BMI1 inhibited cell growth and proliferation**(Figure. 3F, Figure. 4E)**. SPEC-2 cell colony formation assays also showed that high BMI1 expression promoted cell growth and proliferation **(Figure. S4D)**.

4. The synergic anti-growth effect of shBMI1 combine with PTX treatment

PTX is a commonly used chemotherapeutic drug that has a certain effect on the development of CC and EC. To determine the potential functional role of BMI1 in PTX resistance, we transfected with empty plasmids and shBMI1 plasmids in HeLa and HEC-1-A cells. Next, we added PTX (5 nmol/L) after transfected plasmids and shBMI1 plasmids 24 hours. Then, the effect of co-treatment of shBMI1 and 5 nmol/L PTX on cell migration was assessed using a transwell assay. The results showed that after 24 hours of culture, compare with respective control, shBMI1 inhibited the migration of HeLa and HEC-1-A cells, and co-treatment of shBMI1 and 5 nmol/L PTX has a more significant decrease in cell migration of HeLa and HEC-1-A cells (**Figure. 5A, Figure. 6A**). Then, we used a CCK-8 assay to detect the growth and proliferation of HeLa and HEC-1-A cells treated with PTX. The results of the CCK-8 assay showed that cell growth and proliferation were decreased in shBMI1-transfected HeLa and HEC-1-A cells compared with the respective controls. Importantly, the growth and proliferation of shBMI1-transfected HeLa and HEC-1-A cells treated with 5 nmol/L PTX further decreased **(Figure. 5B, Figure. 6B)**. Similarly, in colony formation assay, the number of average colonies counts of shBMI1 knockdown group of HeLa and HEC-1-A cells was apparently lower than respective control, and the co-treatment of shBMI1 and 5 nmol/L PTX has a more significant decrease in cell colony formation **(Figure. 5C, Figure. 6C)**. These results suggest that BMI1 knockdown may be sensitive to the PTX.

Discussion

High BMI1 expression is significantly associated with poor tumor differentiation, high clinical grade, lymph node metastasis, and poor prognosis of CC and EC and is an independent prognostic factor in CC[16]. In line with this evidence, our results also show that the protein level of BMI1 is overexpressed in CC and EC and supports the oncogenic role of BMI1 in the proliferation and migration of CC and EC cells. Moreover, co-administration of PTX and BMI1 inhibition could significantly attenuate the viability of CC and EC cells, indicating a potential target treatment strategy for patients with high BMI1 expression.

Importantly, the pathological evidence that leads to the overexpression of BMI1 in EC and CC remains unknown. On the one hand, there is advancing evidence indicating that BMI1 could be regulated by some miRNAs, a group of endogenous noncoding single-stranded RNAs that negatively regulate the expression of BMI1 genes in several malignant tumors but without CC and EC. We further detected these miRNAs using the GEO database. Indeed, miR-203 was significantly downregulated in CC **(Table S3).** This may lead to high BMI1 expression in CC. The relationship between miR-203 and BMI1 in CC warrants further investigation other miRNAs, such as miR-200 and miR-218, in CC and EC were not similar to previous findings in other cancers[18-21] **(Table S3)**. However, there are limited reports indicating post-translational modification (PTM)-mediated regulation of BMI1, such as ubiquitination, which requires urgent exploration in the future.

Most patients with CC and EC are effectively treated with surgery in the early stages. However, patients with advanced or recurrent disease show a high rate of chemoresistance. To improve drug response rates, strategies for development of more effective and efficient therapy are urgently needed in this field. The link between BMI1 and chemoresistance has been elaborated in several cancers, including head and neck squamous cell carcinoma (HNSCC). The idea that cancer stem-like cells (CSCs) drive cancer metastasis and chemoresistance is well established. For instance, the direct inhibition of BMI1 abrogates the self-renewal process of head and neck cancer stem cells and increases tumor sensitivity to cisplatin[22]. We and others have shown that BMI1 knockdown can increase the efficiency of drugs without an explicit explanation. Only one report has shown that inhibition of BMI1 reduces the migration and invasion of EC cells in vivo and in vitro by upregulating the expression levels of E-cadherin and downregulating N-cadherin, vimentin, and SLUG. Therefore, the underlying mechanism of BMI1-associated drug resistance requires further exploration in CC and EC.

The BMI1 inhibitor, from first-generation PTC-209 to second-generation PTC-028, shows potential effects on the inhibition of cancer cell viability[11; 12]. Although the roles of several key inhibitors have been comprehensively summarized in different tumor cell models, only one inhibitor has been tested in CC and EC respectively[23]. Notably, PTC-596 is the only one BMI1 inhibitor now in the clinical phase 1 trial of diffuse intrinsic pontine glioma and leiomyosarcoma[24; 25], but there is a lack of a unique drug to be used in clinical practice to target BMI1 specifically. Moreover, from the laboratory bench to the clinical bed, the effective function and toxic side effects should also be considered in a carcinosarcoma xenograft model.

Declarations

Acknowledgements

We acknowledge Ms. Zhenzhen Dai(958025950@qq.com) and Mr. Laifu Fang(12576890@qq.com) from The Affiliated People's Hospital of Ningbo University for their technical assistance in the analysis of IHC scores.

Funding

This research was funded by The Medical and health science and Technology project of Zhejiang Province (Grant No.2019337934),

The National Natural Science Foundation of China (Grant No.32270821),

The Natural Science Foundation of Ningbo (Grant No.2021J065 and 2021J017),

The Fundamental Research Funds for the Provincial Universities of Zhejiang (Grant No. SJLZ2022004), and The K.C. Wong Magna Fund in Ningbo University.

Authors' contributions

Yiting Zhao was responsible for clinical data statistics, immunohistochemical experiments, and related data analysis. Yan Lin was responsible for in vitro cell experiments and data analysis. Weili Yang collected the cervical and endometrial cancer samples. Yiting Zhao, Yan Lin and Weili Yang drafted the manuscript. Xiaofeng Jin and Jun Chen made substantial contributions to designing the study and critically revising it for important intellectual content. All authors have read and approved the final manuscript.

Declaration of Competing Interest

The authors declare that they have no competing financial interests or personal relationships that could have influenced the work reported in this study.

Ethical approval

This article does not contain any studies with animals performed by any of the authors.

Consent to participate

Informed consent was obtained from all individual participants included in the study.

Consent to publish

All participants agreed to publish the manuscript.

Data Availability Statements

The datasets analysed during the current study are available in the UCSC platform (https://xenabrowser.net/) and UALCAN platform (http://ualcan.path.uab.edu/index.html) repository.

Address correspondence to

Professor Xiaofeng Jin, Department of Biochemistry and Molecular Biology; Zhejiang Key Laboratory of Pathophysiology, Medical School of Ningbo University, Ningbo, Zhejiang 315211, P.R. China E-mail: jinxiaofeng@nbu.edu.cn

References

1. Y. Liu, P. Fan, Y. Yang, C. Xu, Y. Huang, D. Li, Q. Qing, C. Sun, and H. Zhou, Human papillomavirus and human telomerase RNA component gene in cervical cancer progression. Sci Rep 9 (2019) 15926.https://doi.org/10.1038/s41598-019-52195-5
2. F. Bray, J. Ferlay, I. Soerjomataram, R.L. Siegel, L.A. Torre, and A. Jemal, Global cancer statistics 2018: GLOBOCAN estimates of incidence and mortality worldwide for 36 cancers in 185 countries. CA Cancer J Clin 68 (2018) 394-424.https://doi.org/10.3322/caac.21492
3. R.L. Siegel, K.D. Miller, and A. Jemal, Cancer statistics, 2019. CA Cancer J Clin 69 (2019) 7-34.https://doi.org/10.3322/caac.21551
4. F.S. Falcetta, L.R. Medeiros, M.I. Edelweiss, P.R. Pohlmann, A.T. Stein, and D.D. Rosa, Adjuvant platinum-based chemotherapy for early stage cervical cancer. Cochrane Database Syst Rev 11 (2016) Cd005342.https://doi.org/10.1002/14651858.CD005342.pub4
5. N.R. Datta, E. Stutz, S. Gomez, and S. Bodis, Efficacy and Safety Evaluation of the Various Therapeutic Options in Locally Advanced Cervix Cancer: A Systematic Review and Network Meta-Analysis of Randomized Clinical Trials. Int J Radiat Oncol Biol Phys 103 (2019) 411-437.https://doi.org/10.1016/j.ijrobp.2018.09.037
6. F.Y. Alqahtani, F.S. Aleanizy, E. El Tahir, H.M. Alkahtani, and B.T. AlQuadeib, Paclitaxel. Profiles Drug Subst Excip Relat Methodol 44 (2019) 205-238.https://doi.org/10.1016/bs.podrm.2018.11.001
7. G.V. Glinsky, O. Berezovska, and A.B. Glinskii, Microarray analysis identifies a death-from-cancer signature predicting therapy failure in patients with multiple types of cancer. J Clin Invest 115 (2005) 1503-21.https://doi.org/10.1172/jci23412
8. V. Häyry, O. Tynninen, H.K. Haapasalo, J. Wölfer, W. Paulus, M. Hasselblatt, H. Sariola, A. Paetau, S. Sarna, M. Niemelä, K. Wartiovaara, and N.N. Nupponen, Stem cell protein BMI-1 is an independent marker for poor prognosis in oligodendroglial tumours. Neuropathol Appl Neurobiol 34 (2008) 555-63.https://doi.org/10.1111/j.1365-2990.2008.00949.x
9. R. Bhattacharya, M. Nicoloso, R. Arvizo, E. Wang, A. Cortez, S. Rossi, G.A. Calin, and P. Mukherjee, MiR-15a and MiR-16 control Bmi-1 expression in ovarian cancer. Cancer Res 69 (2009) 9090-5.https://doi.org/10.1158/0008-5472.Can-09-2552

10. M.J. Hoenerhoff, I. Chu, D. Barkan, Z.Y. Liu, S. Datta, G.P. Dimri, and J.E. Green, BMI1 cooperates with H-RAS to induce an aggressive breast cancer phenotype with brain metastases. Oncogene 28 (2009) 3022-32.https://doi.org/10.1038/onc.2009.165
11. A. Kreso, P. van Galen, N.M. Pedley, E. Lima-Fernandes, C. Frelin, T. Davis, L. Cao, R. Baiazitov, W. Du, N. Sydorenko, Y.C. Moon, L. Gibson, Y. Wang, C. Leung, N.N. Iscove, C.H. Arrowsmith, E. Szentgyorgyi, S. Gallinger, J.E. Dick, and C.A. O'Brien, Self-renewal as a therapeutic target in human colorectal cancer. Nat Med 20 (2014) 29-36.https://doi.org/10.1038/nm.3418
12. M. Buechel, A. Dey, S.K.D. Dwivedi, A. Crim, K. Ding, R. Zhang, P. Mukherjee, K.N. Moore, L. Cao, A. Branstrom, M. Weetall, J. Baird, and R. Bhattacharya, Inhibition of BMI1, a Therapeutic Approach in Endometrial Cancer. Mol Cancer Ther 17 (2018) 2136-2143.https://doi.org/10.1158/1535-7163.Mct-17-1192
13. R. Xu, L. Chen, and W.T. Yang, Aberrantly elevated Bmi1 promotes cervical cancer tumorigenicity and tumor sphere formation via enhanced transcriptional regulation of Sox2 genes. Oncol Rep 42 (2019) 688-696.https://doi.org/10.3892/or.2019.7188
14. J. Li, Z. Vangundy, and M. Poi, PTC209, a Specific Inhibitor of BMI1, Promotes Cell Cycle Arrest and Apoptosis in Cervical Cancer Cell Lines. Anticancer Res 40 (2020) 133-141.https://doi.org/10.21873/anticanres.13934
15. A. Zaczek, P. Jóźwiak, P. Ciesielski, E. Forma, K. Wójcik-Krowiranda, Ł. Cwonda, A. Bieńkiewicz, M. Bryś, and A. Krześlak, Relationship between polycomb-group protein BMI-1 and phosphatases regulating AKT phosphorylation level in endometrial cancer. J Cell Mol Med 24 (2020) 1300-1310.https://doi.org/10.1111/jcmm.14782
16. X. Sun, H. Xu, T. Dai, L. Xie, Q. Zhao, X. Hao, Y. Sun, X. Wang, N. Jiang, and M. Sang, Alantolactone inhibits cervical cancer progression by downregulating BMI1. Sci Rep 11 (2021) 9251.https://doi.org/10.1038/s41598-021-87781-z
17. X. Jin, J. Wang, Q. Li, H. Zhuang, J. Yang, Z. Lin, T. Lin, Z. Lv, L. Shen, C. Yan, J. Zheng, J. Zhu, Z. Gong, C. Wang, and K. Gao, SPOP targets oncogenic protein ZBTB3 for destruction to suppress endometrial cancer. Am J Cancer Res 9 (2019) 2797-2812
18. J. Wu, Z.M. Jiang, Y. Xie, X.Q. He, X.H. Lin, J.L. Hu, and Y.Z. Peng, miR-218 suppresses the growth of hepatocellular carcinoma by inhibiting the expression of proto-oncogene Bmi-1. J buon 23 (2018) 604-610
19. W.M. Fu, L.P. Tang, X. Zhu, Y.F. Lu, Y.L. Zhang, W.Y. Lee, H. Wang, Y. Yu, W.C. Liang, C.H. Ko, H.X. Xu, H.F. Kung, and J.F. Zhang, MiR-218-targeting-Bmi-1 mediates the suppressive effect of 1,6,7-trihydroxyxanthone on liver cancer cells. Apoptosis 20 (2015) 75-82.https://doi.org/10.1007/s10495-014-1047-3
20. L. Xu, J. Lin, W. Deng, W. Luo, Y. Huang, C.Q. Liu, F.P. Zhang, Y.F. Qin, P.P. Wong, and C. Liu, EZH2 facilitates BMI1-dependent hepatocarcinogenesis through epigenetically silencing microRNA-200c. Oncogenesis 9 (2020) 101.https://doi.org/10.1038/s41389-020-00284-w

21. Z. Xu, Z. Zhou, J. Zhang, F. Xuan, M. Fan, D. Zhou, Z. Liuyang, X. Ma, Y. Hong, Y. Wang, S. Sharma, Q. Dong, and G. Wang, Targeting BMI-1-mediated epithelial-mesenchymal transition to inhibit colorectal cancer liver metastasis. Acta Pharm Sin B 11 (2021) 1274-1285.https://doi.org/10.1016/j.apsb.2020.11.018
22. A.E. Herzog, K.A. Warner, Z. Zhang, E. Bellile, M.A. Bhagat, R.M. Castilho, G.T. Wolf, P.J. Polverini, A.T. Pearson, and J.E. Nör, The IL-6R and Bmi-1 axis controls self-renewal and chemoresistance of head and neck cancer stem cells. Cell Death Dis 12 (2021) 988.https://doi.org/10.1038/s41419-021-04268-5
23. J. Xu, L. Li, P. Shi, H. Cui, and L. Yang, The Crucial Roles of Bmi-1 in Cancer: Implications in Pathogenesis, Metastasis, Drug Resistance, and Targeted Therapies. Int J Mol Sci 23 (2022).https://doi.org/10.3390/ijms23158231
24. F. Jernigan, A. Branstrom, J.D. Baird, L. Cao, M. Dali, B. Furia, M.J. Kim, K. O'Keefe, R. Kong, O.L. Laskin, J.M. Colacino, M. Pykett, A. Mollin, J. Sheedy, M. Dumble, Y.C. Moon, R. Sheridan, T. Mühlethaler, R.J. Spiegel, A.E. Prota, M.O. Steinmetz, and M. Weetall, Preclinical and Early Clinical Development of PTC596, a Novel Small-Molecule Tubulin-Binding Agent. Mol Cancer Ther 20 (2021) 1846-1857.https://doi.org/10.1158/1535-7163.Mct-20-0774
25. G.I. Shapiro, E. O'Mara, O.L. Laskin, L. Gao, J.D. Baird, R.J. Spiegel, D. Kaushik, M. Weetall, J. Colacino, K. O'Keefe, A. Branstrom, E. Goodwin, J. Infante, P.L. Bedard, and R. Kong, Pharmacokinetics and Safety of PTC596, a Novel Tubulin-Binding Agent, in Subjects With Advanced Solid Tumors. Clin Pharmacol Drug Dev 10 (2021) 940-949.https://doi.org/10.1002/cpdd.904

Tables

Table 1 is available in the Supplementary Files section.

Table 2: Protein level and clinical value of BMI1 in EC

Variables	Number	BMI1, n(%)			χ^2	*P* value
		Negative	Low	High		
Age(years)					2.000	0.368
<50	2	0(0.00)	1(50.0%)	1(50.0%)		
≥50	10	1(10.0%)	1(10.0%)	8(80.0%)		
Height(cm)					1.543	0.462
<=160	7	1(14.00%)	1(14.00%)	5(71.4%)		
>160	5	0(0.00)	2(40.0%)	3(60.0%)		
Weight(KG)					1.029	0.598
<=60	5	0(00.0%)	1(20.00%)	4(80.00%)		
>60	7	1(14.00%)	2(28.50%)	4(57.10%)		
BMI					1.717	0.424
<24	5	1(20.00%)	1(20.00%)	3(60.00%)		
>=24	7	0(0.00)	1(14.00%)	6(86.00%)		
Race					-	-
Asian	12	1(8.30%)	2(16.60%)	9(75%)		
White	0	0(0.00)	0(0.00)	0(0.00)		
Black and African	0	0(0.00)	0(0.00)	0(0.00)		
Tumor size (cm)					2.000	0.368
<4	2	0(0.00)	1(50.0%)	1(50.0%)		
≥4	10	1(10.0%)	1(10.0%)	8(80.0%)		
Infiltrating depth					2.857	0.240
<1/2 depth	5	1(10.0%)	0(0.00)	4(80.0%)		
≥1/2 depth	7	0(0.00)	2(28.5%)	5(71.4%)		
Differentiation					0.800	0.670
Poor	10	1(10.0%)	2(20.0%)	7(70.0%)		
Moderate-High	2	0(0.00)	0(0.00)	2(100%)		
TNM stage					0.800	0.670
I	10	1(10.0%)	2(20.0%)	7(70.0%)		
II	2	0(0.00)	0(0.00)	2(100%)		

FIGO stage					0.800	0.670
I	10	1(10.0%)	2(20.0%)	7(70.0%)		
II	2	0(0.00)	0(0.00)	2(100%)		
ER					-	-
negative	0	0(0.00)	0(0.00)	0(0.00)		
positive	9	0(0.00)	0(0.00)	9(100%)		
P16					-	-
negative	0	0(0.00)	0(0.00)	0(0.00)		
positive	10	0(0.00)	1(10%)	9(90%)		

Figures

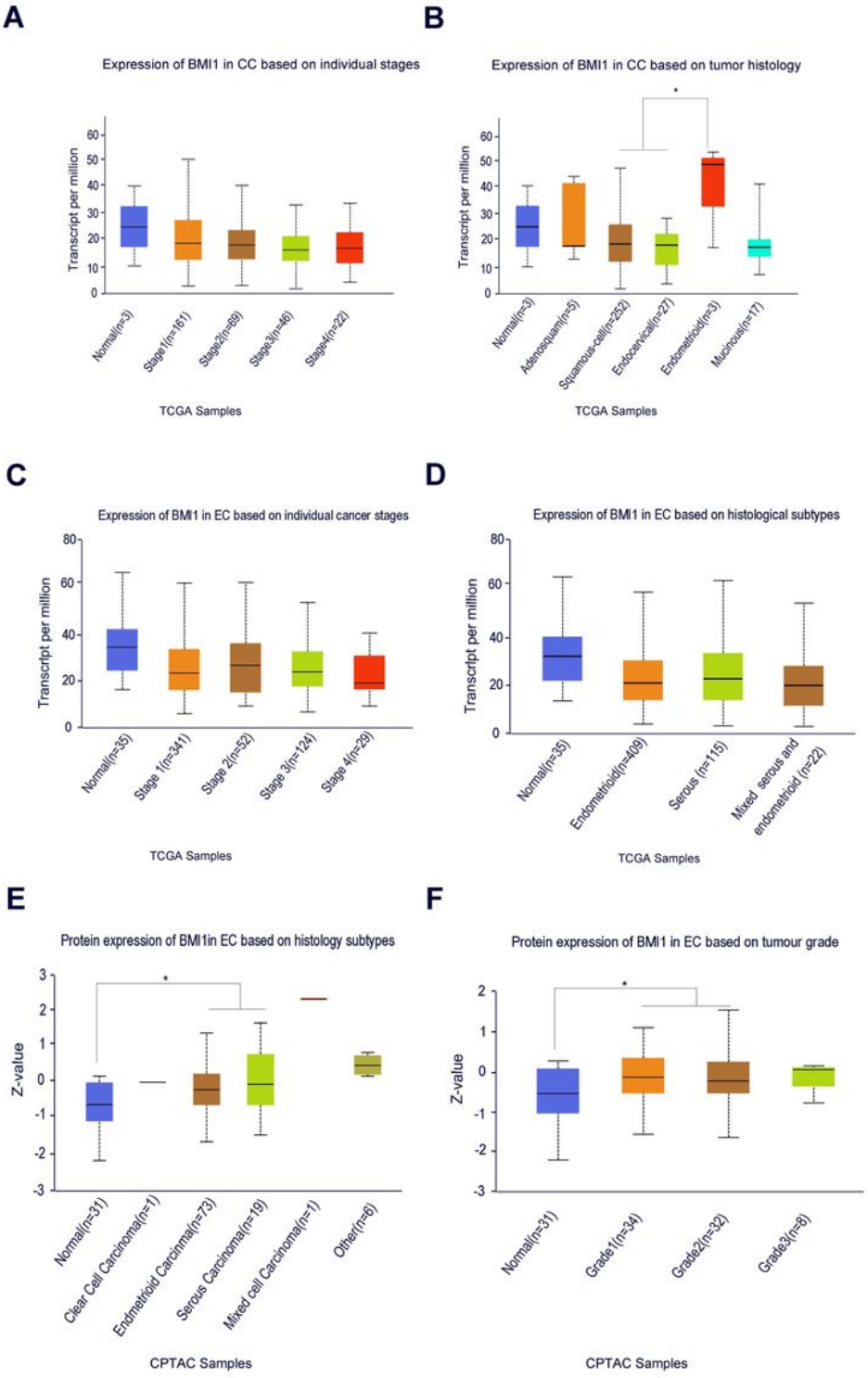

Figure 1

The correlation between BMI1 expression and clinical features in CC and EC.

(A) The expression of BMI1 in CC based on individual stages from TCGA database. The expression of BMI1 was not significantly correlated with the tumor stage of CC. (B) The expression of BMI1 in CC based on tumor histology from the TCGA database. The expression of BMI1 was significantly increased in the

endometrioid adenocarcinoma subtype of CC compared to the squamous cell and endocervical subtypes. *P<0.05. (C) The expression of BMI1 in EC based on individual stages from TCGA database. (D) Expression of BMI1 in EC based on histology subtypes from TCGA database. (E) Protein expression of BMI1 in EC based on histology subtypes from the CPTAC database. BMI1 protein expression was higher in EC tissues than that in normal tissues. * P<0.05. (F) Protein expression of BMI1 in EC based on tumor grade from the CPTAC database. BMI1 protein is highly expressed in endometrioid carcinoma subtype and serous carcinoma subtype compared with normal tissues. *P < 0.05.

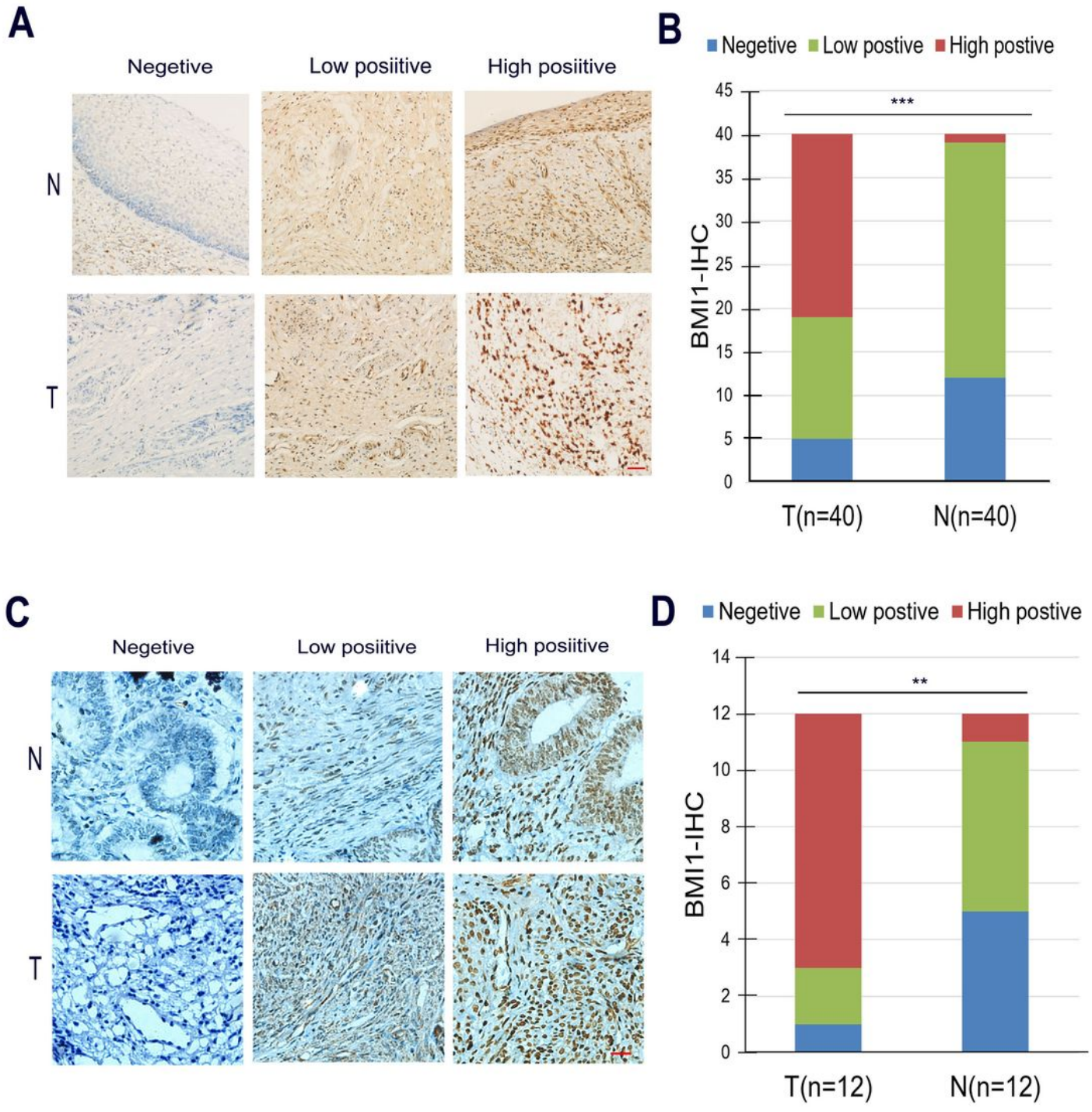

Figure 2

BMI1 protein expression is elevated in CC and CE specimens.

(A) Representative images of BMI1 IHC from 40 cases of CC specimens. Scale bar, 200 μm. (B) Quantitative data of BMI1 protein staining in A. Statistical significance was determined by chi-square test. ***P < 0.001. (C) Representative images of BMI1 IHC from 12 cases of CE specimens. Scale bar, 200 μm. (D) Quantitative data of BMI1 protein staining in C. Statistical significance was determined by chi-square test. ** P < 0.01.

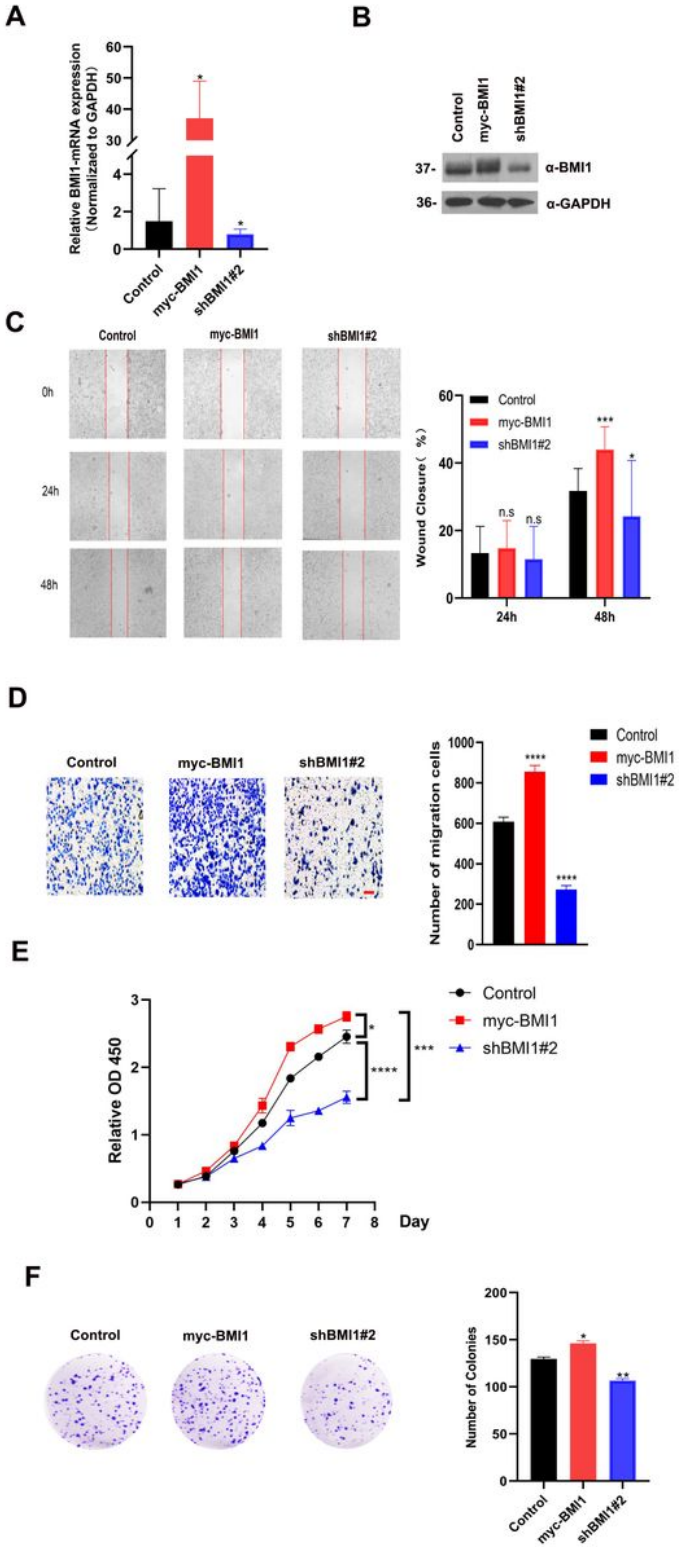

Figure 3

Effect of BMI1 on the growth proliferation and migration invasion of HeLa cervical cancer cells.

(A) RT-qPCR measured BMI1 gene mRNA expression in control, myc-BMI1 high expression group, and shBMI1 knockdown group of HeLa cells. Data are shown as means ± SD (n=3). *P < 0.05. (B) Western blot of HeLa cells transfected with empty plasmids myc-BMI1 and shBMI1#2 plasmids. (C) Wound

healing at 24h and 48h in the wound-healing closure assay; Statistical analysis of wound healing area data are shown as means ± SD (n=3). *P < 0.05. (D) Transwell migration assay of HeLa cells transfected with empty plasmids myc-BMI1 and shBMI1#2 plasmids. Statistical analysis of transwell assay was performed using one-way ANOVA. **P < 0.001. Scale bar, 200 μm. (E) Cell proliferation assay of HeLa cells transfected with empty plasmids, myc-BMI1 and shBMI1#2 plasmids. (F) Cell colony formation assay of HeLa cells transfected with empty plasmids, myc-BMI1 and shBMI1#2 plasmids, all data shown are mean values ± SD (n=3). *P < 0.05.

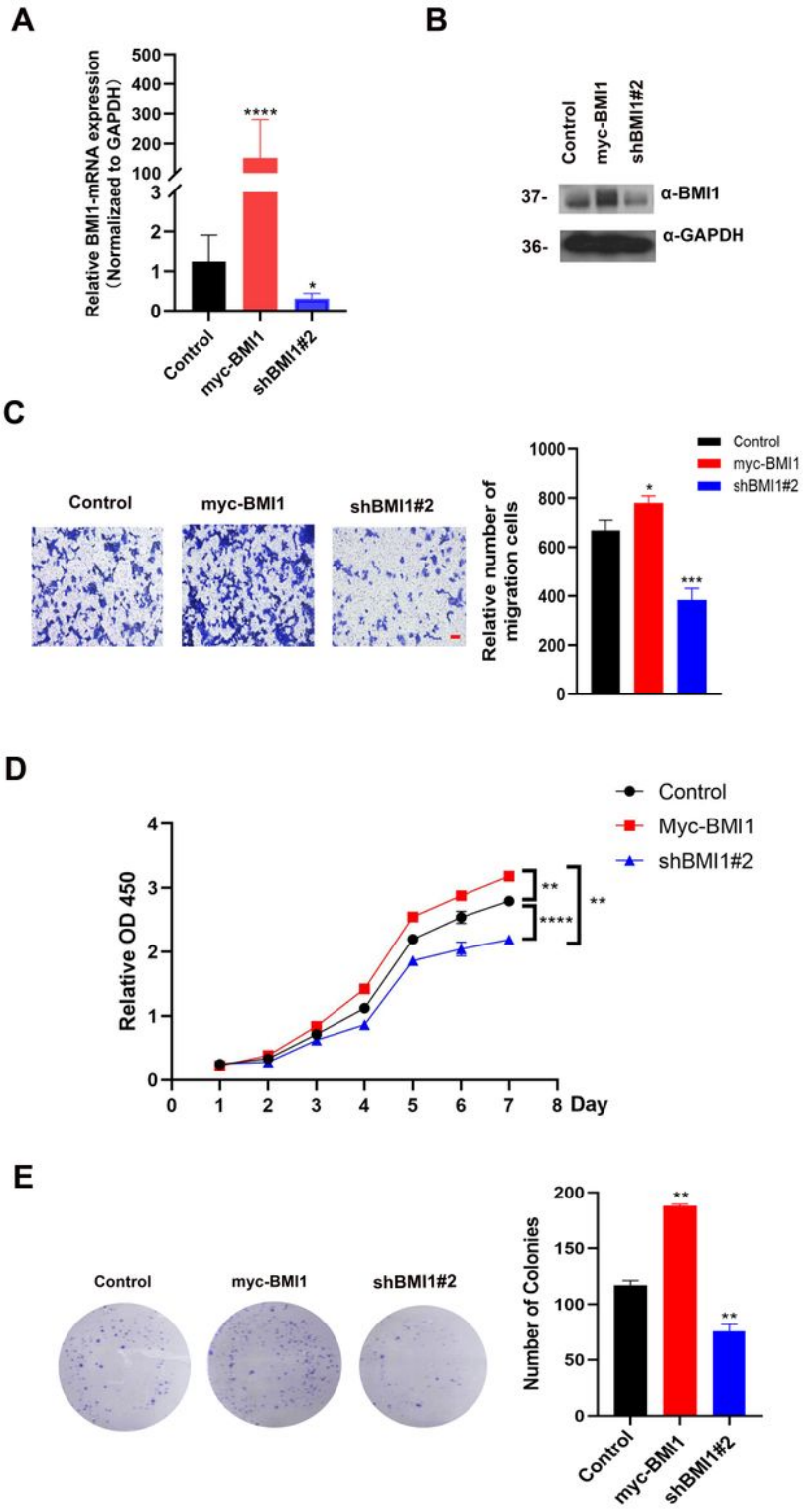

Figure 4

Effect of BMI1 on the growth proliferation and migration invasion of HEC-1-A endometrial cancer cells.

(A) RT-qPCR measured BMI1 gene mRNA expression in control, myc-BMI1 high expression group and shBMI1 knockdown group of HEC-1-A cells, data are shown as means ± SD (n=3). *P < 0.05. (B) Western blot of HEC-1-A cells transfected with empty plasmids, myc-BMI1 and shBMI1#2 plasmids. (C) Transwell migration assay of HEC-1-A cells transfected with empty plasmids myc-BMI1 and shBMI1#2 plasmids, Scale bar, 200 μm. (D) Cell proliferation assay of HEC-1-A cells transfected with empty plasmids, myc-BMI1 and shBMI1#2 plasmids. Statistical analysis was performed using one-way ANOVA. *P < 0.05. (E) Cell colony formation assay of HEC-1-A cells transfected with empty plasmids and myc-BMI1 plasmids, all data shown are mean values ± SD (n=3). *P < 0.05.

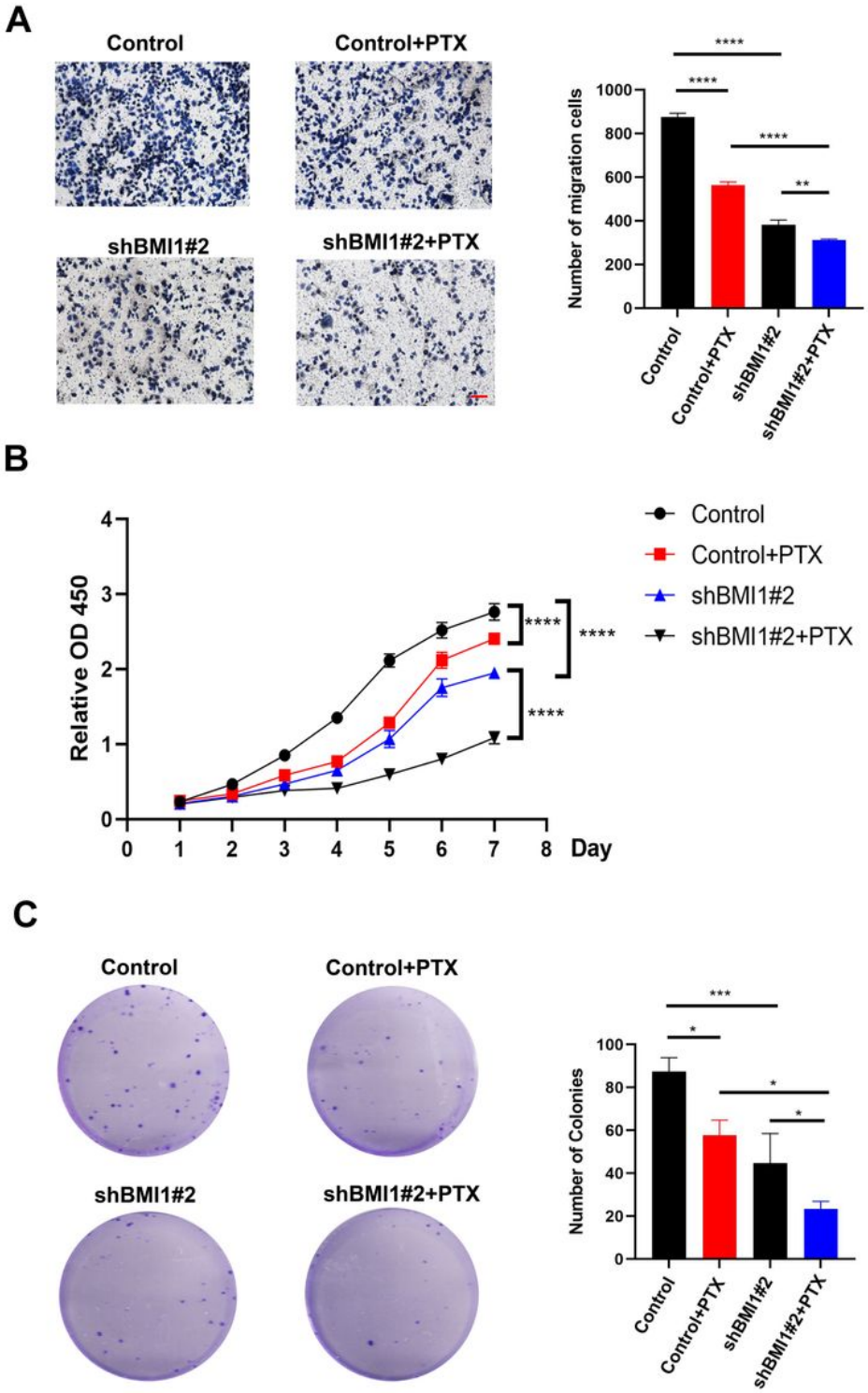

Figure 5

BMI1 expression promotes paclitaxel (PTX) resistance in HeLa cervical cancer cells.

(A) Transwell migration assay of HeLacells transfected with empty plasmids and shBMI1#2 plasmids. 5nmol/L PTX was added after transfected 24hours. Statistical analysis was performed using one-way ANOVA. *P < 0.05; Scale bar, 200 μm. (B) Cell proliferation assay of HeLa cells transfected with empty

plasmids andshBMI1#2 plasmids. 5nmol/L PTX was added after transfected 24hours. Statistical analysis was performed using one-way ANOVA. *P < 0.05. (C) Cell colony formation assay of HeLa cells transfected with empty plasmids andshBMI1#2 plasmids. 5nmol/L PTX was added after transfected 24hours, all data shown are mean values ± SD (n=3). *P < 0.05.

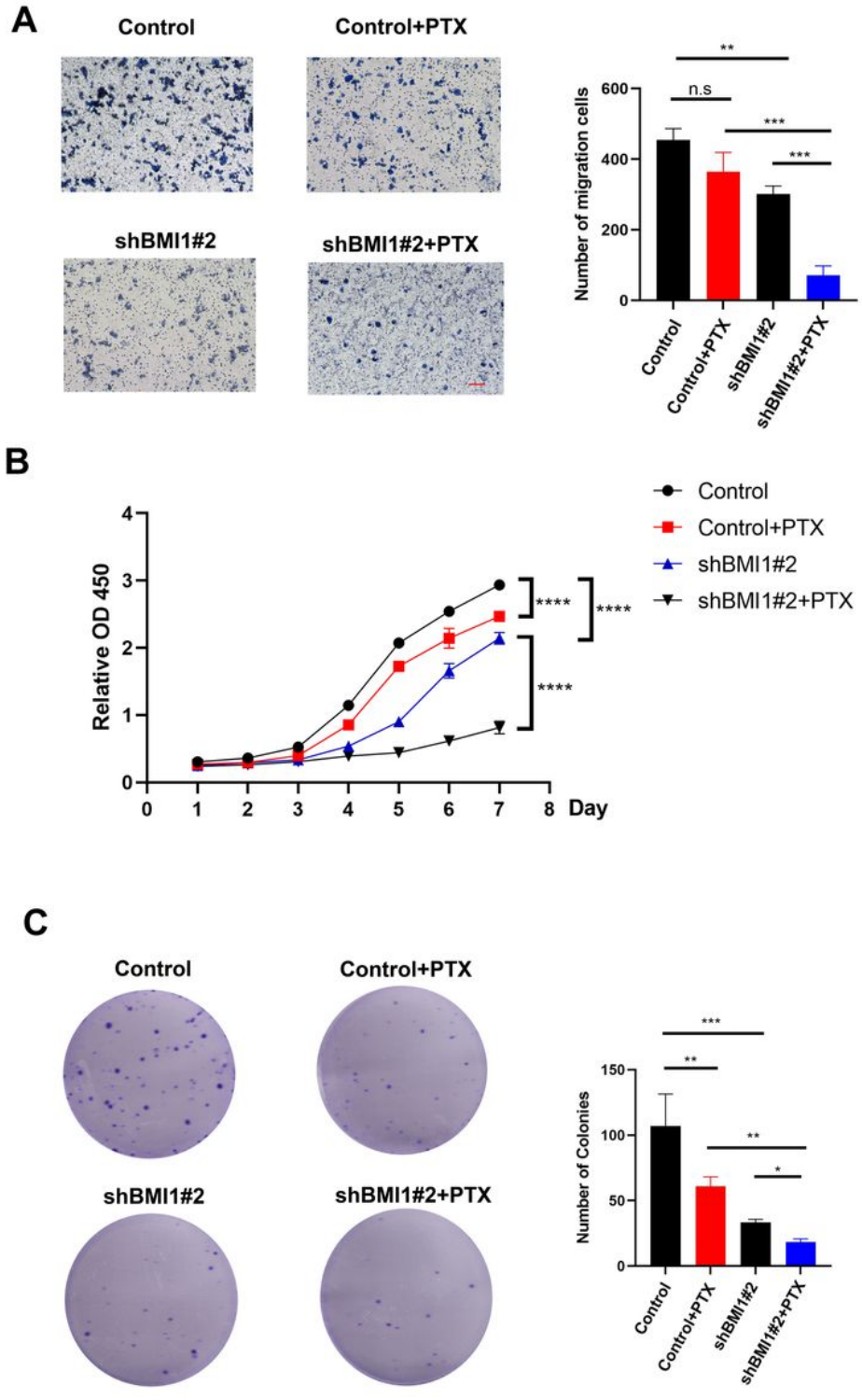

Figure 6

BMI1 expression promotes paclitaxel (PTX) resistance in HEC-1-A endometrial cancer cells.

(A) Transwell migration assay of HEC-1-Acells transfected with empty plasmids and shBMI1#2 plasmids. 5nmol/L PTX was added after transfected 24hours. Statistical analysis was performed using one-way ANOVA. *P < 0.05; Scale bar, 200 μm. (B) Cell proliferation assay of HEC-1-A cells transfected with empty plasmids andshBMI1#2 plasmids. 5nmol/L PTX was added after transfected 24hours. Statistical analysis was performed using one-way ANOVA. *P < 0.05. (C) Cell colony formation assay of HEC-1-A cells transfected with empty plasmids andshBMI1#2 plasmids. 5nmol/L PTX was added after transfected 24hours, all data shown are mean values ± SD (n=3). *P < 0.05.

Supplementary Files

This is a list of supplementary files associated with this preprint. Click to download.

- Table1.docx
- Supplementarymaterials.docx